Theory of multiphonon excitation in heavy-ion collisions

C. A. Bertulani and L. F. Canto
Instituto de Física, Universidade Federal do Rio de Janeiro, Caixa Postal 68528, 21945-970 Rio de Janeiro, Rio de Janeiro, Brazil

M. S. Hussein*
Center for Theoretical Physics, Laboratory for Nuclear Science and Department of Physics, Massachusetts Institute of Technology, Cambridge, Massachusetts 02139
and Institute for Theoretical Atomic and Molecular Physics at the Harvard-Smithsonian Center for Astrophysics, 60 Graden Street, Cambridge, Massachusetts 02138

A. F. R. de Toledo Piza
Instituto de Física, Universidade de São Paulo, Caixa Postal 66318, 05389-970 São Paulo, SP, Brazil
(Received 13 July 1995)

We study the effects of channel coupling in the excitation dynamics of giant resonances in relativistic heavy ions collisions. For this purpose, we use a semiclassical approximation to the coupled-channels problem and separate the Coulomb and the nuclear parts of the coupling into their main multipole components. In order to assess the importance of multistep processes, we neglect the resonance widths and solve the set of coupled equations exactly. Finite widths are then considered. In this case, we handle the coupling of the ground state with the dominant giant dipole resonance exactly and study the excitation of the remaining resonances within the coupled-channels Born approximation. A comparison with recent experimental data is made.

PACS number(s): 24.30.Cz, 24.10.Eq, 21.10.Re

I. INTRODUCTION

Relativistic Coulomb excitation (RCE) is a well established tool to unravel interesting aspects of nuclear structure [1]. Examples are the studies of multiphonon resonances in the SIS accelerator at the GSI facility, in Darmstadt, Germany [2,3]. Important properties of nuclei far from stability [4] have also been studied with this method. The RCE induced by large-Z projectiles and/or targets, often yields large cross sections in grazing colisions. This results from the large nuclear response (in the region of the giant resonances) to the acting electromagnetic fields. As a consequence, a strong coupling between the excited states is expected This coupling might be responsible for the large discrepancies between experimental data of RCE and the calculations based on first-order perturbation theory [1–3], or the harmonic oscillator model.

In the present paper, we apply a semiclassical method [5] to the coupled-channels (CC) problem and study RCE in several collisions between heavy ions. In this method, the projectile-target relative motion is approximated by a classical trajectory and the excitation of the giant resonances is treated quantum mechanically [6,7]. The use of this method is justified due to the small wavelengths associated with the relative motion. In Sec. II, we neglect the resonance widths and introduce the semiclassical CC equations for relativistic Coulomb excitation. The time-dependent matrix elements of the main multipole components of the Coulomb (Sec. II A) and nuclear (Sec. II B) parts of the coupling interaction are calculated. The CC equations are then solved in some limiting cases. Section III is devoted to the excitation of resonances of finite widths. Generalizing the schematic treatment of Ref. [6], we present an ''exact'' solution for the coupling between the ground state (g.s.) and the dominant GDR. The excitation of the weaker resonances are then evaluated through the coupled-channels Born approximation (CCBA), from the g.s. and GDR amplitudes. In Sec. IV we apply the results of the previous sections to specific cases and make a comparison with recent experimental data. Finally, in Sec. V, we summarize our results and present the conclusions of this work.

II. THE SEMICLASSICAL METHOD FOR THE CC-PROBLEM

In relativistic heavy ion collisions, the wavelength associated to the projectile-target separation is much smaller than the characteristic lengths of system. It is, therefore, a reasonable approximation to treat $\mathbf{r}$ as a classical variable $\mathbf{r}(t)$, given at each instant by the trajectory followed by the relative motion. At high energies, it is also a good approximation to replace this trajectory by a straight line. The intrinsic dynamics can then be handled as a quantum mechanics problem with a time dependent Hamiltonian. This treatment is discussed in full details by Alder and Winther in Ref. [5].

The intrinsic state $|\psi(t)\rangle$ satisfies the Schrödinger equation

$$[H+V(\mathbf{r}(t))]|\psi(t)\rangle = i\hbar \frac{\partial|\psi(t)\rangle}{\partial t}. \tag{1}$$

Above, H is the intrinsic Hamiltonian and V is the channel-coupling interaction.

*Permanent address: Instituto de Fisica, Universidade de São Paulo, Cx. Postal 66318, 05389-970 São Paulo, SP, Brazil.

Expanding the wave function in the set $\{|m\rangle;\ m=0,N\}$ of eigenstates of H, where N is the number of excited states included in the coupled-channel problem, we obtain

$$|\psi(t)\rangle=\sum_{m=0}^{N} a_m(t)|m\rangle\exp(-iE_m t/\hbar), \tag{2}$$

where E_m is the energy of the state $|m\rangle$. Taking scalar product with each of the states $\langle n|$, we get the set of coupled equations

$$i\hbar\dot{a}_n(t)=\sum_{m=0}^{N}\langle n|V|m\rangle e^{i(E_n-E_m)t/\hbar}a_m(t),\quad n=0\text{ to }N. \tag{3}$$

It should be remarked that the amplitudes depend also on the impact parameter b specifying the classical trajectory followed by the system. For the sake of keeping the notation simple, we do not indicate this dependence explicitly. We write, therefore, $a_n(t)$ instead of $a_n(b,t)$. Since the interaction V vanishes as $t\to\pm\infty$, the amplitudes have as initial condition $a_n(t\to-\infty)=\delta(n,0)$ and they tend to constant values as $t\to\infty$. Therefore, the excitation probabity of an intrinsic state $|n\rangle$ in a collision with impact parameter b is given as

$$P_n(b)=|a_n(\infty)|^2. \tag{4}$$

The total cross section for excitation of the state $|n\rangle$ can be approximated by the classical expression

$$\sigma_n=2\pi\int P_n(b)b\,db. \tag{5}$$

Since we are interested in the excitation of specific nuclear states, with good angular momentum and parity quantum numbers, it is appropriate to develop the time-dependent coupling interaction $V(t)$ into multipoles. In Ref. [8], a multipole expansion of the electromagnetic excitation amplitudes in relativistic heavy ion collisions was carried out. This work used first order perturbation theory and the semiclassical approximation. The time dependence of the multipole interactions was not explicitly given. In Sec. II A we show how this time dependence can be explicitly obtained, from the Taylor-series expansion of the Liénard-Wiechert potentials [9] and the continuity equation for the nuclear current.

In Sec. II B we deduce the time dependence and the multipole decomposition of the nuclear interaction in relativistic nucleus-nucleus collisions. The nuclear absorption at collisions below grazing impact parameter is also accounted for.

A. Coulomb excitation

We consider a nucleus 1 which is at rest and a relativistic nucleus 2 which moves along the z axis and is excited from the initial state $|I_iM_i\rangle$ to the state $|I_fM_f\rangle$ by the electromagnetic field of nucleus 1. The nuclear states are specified by the spin quantum numbers I_i, I_f and by the corresponding magnetic quantum numbers M_i and M_f, respectively. We assume that the relativistic nucleus 2 moves along a straight-line trajectory with impact parameter b, which is therefore also the distance of the closest approach between the center of mass of the two nuclei at the time $t=0$. We shall consider the situation where b is larger than the sum of the two nuclear radii, such that the charge distributions of the two nuclei do not strongly overlap at any time. The electromagnetic field of the nucleus 2 in the reference frame of nucleus 1 is given by the usual Lorentz transformation [9] of the scalar potential $\phi(\mathbf{r})=Z_1e/|\mathbf{r}|$, i.e.,

$$\phi(\mathbf{r}',t)=\gamma\phi[\mathbf{b}'-\mathbf{b},\gamma(z'-vt)],$$

$$\mathbf{A}(\mathbf{r}',t)=\frac{\mathbf{v}}{c}\gamma\phi[\mathbf{b}'-\mathbf{b},\gamma(z'-vt)]. \tag{6}$$

Here $\mathbf{b}$ (impact parameter) and $\mathbf{b}'$ are the components of the radius vectors $\mathbf{r}$ and $\mathbf{r}'$ transverse to $\mathbf{v}$.

The time-dependent matrix element for electromagnetic excitation is of the form

$$V_{fi}(t)=\langle I_fM_f|\left[\rho(\mathbf{r}')-\frac{\mathbf{v}}{c^2}\cdot\mathbf{J}(\mathbf{r}')\right]\phi(\mathbf{r}',t)|I_iM_i\rangle. \tag{7}$$

A Taylor-series expansion of the Liénard-Wiechert potential around $\mathbf{r}'=0$ yields

$$\phi(\mathbf{r}',t)=\gamma\phi[\mathbf{r}(t)]+\gamma\nabla\phi[\mathbf{r}(t)]\cdot\mathbf{r}'+\cdots, \tag{8}$$

where $\mathbf{r}=(\mathbf{b},\gamma vt)$, and the following simplifying notation is used:

$$\nabla\phi[\mathbf{r}]\equiv\nabla'\phi(\mathbf{r}',t)|_{\mathbf{r}'=0}=-\nabla_{\mathbf{b}}\phi(\mathbf{r})-\frac{\partial}{\partial(vt)}\phi(\mathbf{r})\hat{\mathbf{z}}$$

$$=-\nabla_{\mathbf{b}}\phi(\mathbf{r})-\frac{\mathbf{v}}{c^2}\frac{\partial}{\partial t}\phi(\mathbf{r}). \tag{9}$$

Thus

$$V_{fi}(t)=\langle I_fM_f|\left[\rho(\mathbf{r}')-\frac{\mathbf{v}}{c^2}\cdot\mathbf{J}(\mathbf{r}')\right]\times[\gamma\phi(\mathbf{r})+\gamma\mathbf{r}'\cdot\nabla\phi(\mathbf{r})]|I_iM_i\rangle. \tag{10}$$

Using the continuity equation

$$\nabla\cdot\mathbf{J}=-i\omega\rho, \tag{11}$$

where $\omega=(E_f-E_i)/\hbar$, and integrating by parts,

$$V_{fi}(t)=\langle I_fM_f|\left\{\mathbf{J}(\mathbf{r})\cdot\left[\frac{\nabla'}{i\omega}-\frac{\mathbf{v}}{c^2}\right]\right\}\times[\gamma\phi(\mathbf{r}+\gamma\mathbf{r}'\cdot\nabla\phi(\mathbf{r})]|I_iM_i\rangle. \tag{12}$$

In spherical coordinates

$$\mathbf{r}'\cdot\nabla\phi=\frac{\sqrt{4\pi}}{3}\sum_{\mu=-1}^{1}\alpha_\mu r'Y_{1\mu}^*, \tag{13}$$

where

$$\alpha_\mu=\hat{\mathbf{e}}_\mu\cdot\nabla\phi, \tag{14}$$

and $\hat{\mathbf{e}}_\mu$ are the spherical unit vectors

$$\hat{\mathbf{e}}_\pm = \mp\frac{1}{\sqrt{2}}(\hat{\mathbf{e}}_X \pm \hat{\mathbf{e}}_Y), \quad \hat{\mathbf{e}}_0 = \hat{\mathbf{e}}_Z .$$

We will use the relations

$$\frac{\mathbf{r}}{c^2} = \frac{v}{c^2}\hat{\mathbf{e}}_0 = \frac{v}{c^2}\sqrt{\frac{4\pi}{3}}\nabla(rY_{10}^*) \tag{15}$$

and

$$\nabla\times\mathbf{L}(r^k Y_{lm}) = i(k+1)\nabla(r^k Y_{lm}), \tag{16}$$

where $\mathbf{L} = -i\mathbf{r}\times\nabla$.

Then, one can write

$$\mathbf{J}\cdot\left(\frac{\nabla}{i\omega} - \frac{\mathbf{v}}{c^2}\right)[\gamma\phi + \gamma\mathbf{r}'\cdot\nabla\phi]$$
$$= -\gamma\mathbf{J}\cdot\left[\frac{\mathbf{v}}{c^2}(\nabla\phi\cdot\mathbf{r}') - \sqrt{\frac{4\pi}{3}}\right.$$
$$\left.\times\left\{\sum_{\mu=-1}^{1}\frac{\alpha_\mu}{i\omega}\nabla'(r'Y_{1\mu}) - \frac{v}{c^2}\phi\nabla'(r'Y_{10}^*)\right\}\right]. \tag{17}$$

The last term in the above equation can be rewritten as

$$\left(\mathbf{J}\cdot\frac{\mathbf{v}}{c^2}\right)(\mathbf{r}'\cdot\nabla\phi) = \frac{v}{2c^2}\mathbf{J}\cdot[\hat{\mathbf{e}}_0(\mathbf{r}'\cdot\nabla\phi) + (\mathbf{r}'\cdot\hat{\mathbf{e}}_0)\nabla\phi]$$
$$+ \frac{v}{2c^2}\mathbf{J}\cdot[\hat{\mathbf{e}}_0(\mathbf{r}'\cdot\nabla\phi) - (\mathbf{r}'\cdot\hat{\mathbf{e}}_0)\nabla\phi]. \tag{18}$$

The first term in this equation is symmetric under parity inversion, and contributes to the electric quadrupole ($E2$) excitation amplitudes, since

$$\frac{v}{2c^2}\mathbf{J}\cdot[\hat{\mathbf{e}}_0(\mathbf{r}'\cdot\nabla\phi) + (\mathbf{r}'\cdot\hat{\mathbf{e}}_0)\nabla\phi] = \frac{v}{2c^2}\mathbf{J}\cdot\nabla'[z'(\mathbf{r}'\cdot\nabla\phi)]. \tag{19}$$

The second term in Eq. (18) is antisymmetric in $\mathbf{J}$ and $\mathbf{r}'$, and leads to magnetic dipole ($M1$) excitations. Indeed, using Eqs. (13)–(16), one finds

$$\frac{v}{2c^2}\mathbf{J}\cdot[\hat{\mathbf{e}}_0(\mathbf{r}'\cdot\nabla\phi) - (\mathbf{r}'\cdot\hat{\mathbf{e}}_0)\nabla\phi]$$
$$= \frac{v}{2c^2}\mathbf{J}\cdot\left[\sqrt{\frac{4\pi}{3}}\sum_{\mu=-1}^{1}\alpha_\mu(-1)^\mu\mathbf{L}(\mathbf{r}Y_{1,-\mu})\right]. \tag{20}$$

Thus only the first two terms on the right-hand side of Eq. (17) contribute to the electric dipole ($E1$) excitations. Inserting them into Eq. (12), we get

$$V_{fi}^{(E1)}(t) = \gamma\sqrt{\frac{4\pi}{3}}\sum_{\mu=-1}^{1}(-1)^\mu\beta_\mu$$
$$\times\langle I_f M_f|\mathscr{M}(E1,-\mu)|I_i M_i\rangle, \tag{21}$$

where

$$\mathscr{M}(E1,-\mu) = \frac{i}{\omega}\int d^3r\,\mathbf{J}(\mathbf{r})\cdot\nabla(rY_{1\mu})$$
$$= \int d^3r\,\rho(\mathbf{r})rY_{1\mu}(\mathbf{r}), \tag{22}$$

and

$$\beta_\pm = -\alpha_\mu = -(\nabla\phi\cdot\hat{\mathbf{e}}_\mu) = \hat{\mathbf{e}}_\mu\cdot\frac{\partial\phi}{\partial\mathbf{b}},$$

$$\beta_0 = -\alpha_0 - i\frac{\omega v}{c^2}\phi. \tag{23}$$

The derivatives of the potential ϕ are explicitly given by

$$\frac{\partial\phi}{\partial\mathbf{b}_x} \equiv \nabla_{\mathbf{b}_x}\phi|_{\mathbf{r}'=0} = -\hat{\mathbf{x}}b_x\frac{Z_1 e}{[b^2+\gamma^2v^2t^2]^{3/2}},$$

$$\nabla_z\phi|_{\mathbf{r}'=0} = -\hat{\mathbf{z}}\gamma^2 vt\frac{Z_1 e}{[b^2+\gamma^2v^2t^2]^{3/2}}. \tag{24}$$

Using the results above, we get for the electric dipole potential

$$V_{fi}^{(E1)}(t) = \sqrt{\frac{2\pi}{3}}\gamma\left\{\mathscr{E}_1(\tau)[\mathscr{M}_{fi}(E1,-1) - \mathscr{M}_{fi}(E1,1)]\right.$$
$$+\sqrt{2}\gamma\tau\left[\mathscr{E}_1(\tau) - i\frac{\omega v b}{c^2}\right.$$
$$\left.\left.\times(1+\tau^2)\mathscr{E}_2(\tau)\right]\mathscr{M}_{fi}(E1,0)\right\}, \tag{25}$$

where $\tau = \gamma v t/b$, and

$$\mathscr{E}_1(\tau) = \frac{Z_1 e}{b^2[1+\tau^2]^{3/2}} \quad \text{and} \quad \mathscr{E}_2(\tau) = \frac{Z_1 e\,\tau}{b[1+\tau^2]^{3/2}} \tag{26}$$

are the transverse and longitudinal eletric fields generated the relativistic nucleus with charge $Z_1 e$, respectively. From the definition

$$\mathscr{M}_{fi}(M1,\mu) = -\frac{i}{2c}\int d^3r\,\mathbf{J}(\mathbf{r})\cdot\mathbf{L}(rY_{1\mu}), \tag{27}$$

and Eq. (19), we find

$$V_{fi}^{(M1)}(t) = i\sqrt{\frac{2\pi}{3}}\frac{v}{c}\mathscr{E}_1(\tau)[\mathscr{M}_{fi}(M1,1) - \mathscr{M}_{fi}(M1,-1)]. \tag{28}$$

The current $\mathbf{J}$ in Eq. (27) is made up of the usual convective part and a magnetization part, proportional to the intrinsic (Dirac and anomalous) magnetic moment of the nucleons.

To obtain the electric quadrupole ($E2$) potential we use the third term in the Taylor expansion of Eq. (8). Using the continuity equation, a part of this term will contribute to $E3$ and $M2$ excitations, which we neglect. We then find that

$$V_{fi}^{(E2)}(\tau)=-\sqrt{\frac{\pi}{30}}\gamma\left\{3\mathscr{E}_3(\tau)[\mathscr{M}_{fi}(E2,2)+\mathscr{M}_{fi}(E2,-2)]+\gamma\left[6\tau\mathscr{E}_3(\tau)-i\frac{\omega v}{\gamma c^2}(1+\tau^2)\mathscr{E}_1(\tau)\right]\right.$$
$$\left.\times[\mathscr{M}_{fi}(E2,-1)+\mathscr{M}_{fi}(E2,1)]+\sqrt{6}\gamma^2\left[(2\tau^2-1)\mathscr{E}_3(\tau)-i\frac{\omega v}{\gamma c^2}\tau(1+\tau^2)\mathscr{E}_1(\tau)\right]\mathscr{M}_{fi}(E2,0)\right\}, \quad (29)$$

where $\mathscr{E}_3(\tau)$ is the quadrupole electric field of nucleus 1, given by

$$\mathscr{E}_3(\tau)=\frac{Z_1 e}{b^3[1+\tau^2]^{5/2}}. \quad (30)$$

The fields $\mathscr{E}_i(\tau)$ peak around $\tau=0$, and decrease fastly within an interval $\Delta\tau\simeq 1$. This corresponds to a collisional time $\Delta t\simeq b/\gamma v$. This means that numerically one needs to integrate the coupled-channels equations [Eq. (3)] only in a time interval within a range $n\times\Delta\tau$ around $\tau=0$, with n equal to a small integer number. This will be shown later in connection with the calculation presented in Sec. IV.

Using the Wigner-Eckart theorem we can write [10]

$$\mathscr{M}_{fi}(E\lambda,\mu)=(-1)^{I_f-M_f}\begin{pmatrix} I_f & \lambda & I_i \\ -M_f & \mu & Mi\end{pmatrix}$$
$$\times\langle I_f M_f||\mathscr{M}(E\lambda)||I_i M_i\rangle. \quad (31)$$

A phase convention for the nuclear states can be found so that the reduced matrix elements $\langle I_f M_f||\mathscr{M}(E\lambda)||I_i M_i\rangle$ are real numbers [5]. For the case of giant resonances, sum rules are very useful to guess the values of these matrix elements. It is usual to use the reduced transition probability

$$B(E\lambda;I_i\rightarrow I_f)=\frac{1}{2I_i+1}\sum_{M_i M_f}|\langle I_i M_i|\mathscr{M}(E\lambda,\mu)|I_f M_f\rangle|^2$$
$$=\frac{1}{2I_i+1}|\langle I_i||\mathscr{M}(E\lambda)||I_f\rangle|^2, \quad (32)$$

in terms of which the energy-weighted sum-rules yield, for the $E1$ and $E2$ excitations,

$$B(E1;I_i\rightarrow I_f)=\left(\frac{1}{2I_f+1}\right)\frac{9}{4\pi}\frac{\hbar^2}{2m_N}\frac{NZ}{AE_x}e^2, \quad (33)$$

and

$$B(E2;I_i\rightarrow I_f)=\left(\frac{1}{2I_f+1}\right)\frac{\hbar^2}{m_N}\frac{15R^2}{4\pi E_x}e^2\times\begin{cases} Z^2/A, & \text{for isoscalar excitations;}\\ NZ/A, & \text{for isovector excitations;}\end{cases} \quad (34)$$

where N, Z, and A are the neutron, charge, and mass number of the excited nucleus, respectively. In these equations it was assumed that an isolated state with energy E_x exhausts the sum rule.

The matrix elements for the transitions between multiphonon states can be determined by using the Wigner-Eckart theorem and the reduced matrix elements inferred from sum rules, as described in Secs. II A and II B. In the case of perfect phonons, i.e., eigenstate solutions of the harmonic oscillator, the following relation holds for the reduced matrix elements for the transition $0\rightarrow 1$ and $n-1\rightarrow n$ [13]:

$$|\langle n-1||V_{E/N,1}||n\rangle|^2=n|\langle 0||V_{E/N,1}||1\rangle|^2. \quad (35)$$

The factor n on the right-hand side (rhs) is the boson enhacement factor.

1. Approximate solutions

In most cases, the first-order perturbation theory is a good approximation to calculate the amplitudes for relativistic Coulomb excitation. It amounts to using $a_k=\delta_{k0}$ on the right-hand side of Eq. (3). The time integrals can be evaluated analytically for the $V_{Ei}(t)$ perturbations, given by Eqs. (25), (28), and (29). The result is

$$a_{1\text{st}}^{(E1)}=-i\sqrt{\frac{8\pi}{3}}\frac{Z_1 e}{\hbar v b}\xi\left\{K_1(\xi)[\mathscr{M}_{fi}(E1,-1)-\mathscr{M}_{fi}(E1,1)]+i\frac{\sqrt{2}}{\gamma}K_0(\xi)\mathscr{M}_{fi}(E1,0)\right\}, \quad (36)$$

where K_1 (K_2) is the modified Bessel function of first (second) degree, and $\xi=\omega b/\gamma v$. For the $E2$ and $M1$ multipolarities, we obtain respectively,

$$a_{1\mathrm{st}}^{(E2)}=2i\sqrt{\frac{\pi}{30}}\frac{Z_1 e}{\gamma\hbar v b^2}\xi^2\Bigg\{K_2(\xi)[\mathcal{M}_{fi}(E2,2)+\mathcal{M}_{fi}(E2,-2)]+i\gamma\left(2-\frac{v^2}{c^2}\right)K_1(\xi)[\mathcal{M}_{fi}(E2,-1)+\mathcal{M}_{fi}(E2,1)]$$
$$-\sqrt{6}K_0(\xi)\mathcal{M}_{fi}(E2,0)\Bigg\}, \tag{37}$$

and

$$a_{1\mathrm{st}}^{(M1)}=\sqrt{\frac{8\pi}{3}}\frac{Z_1 e}{\hbar c b}\xi K_1(\xi)[\mathcal{M}_{fi}(M1,1)-\mathcal{M}_{fi}(M1,-1)]. \tag{38}$$

These expressions are the same as those obtained from the formulas deduced in Ref. [8]. We note that the multipole decomposition developed by those authors is accomplished by a different approach, i.e., using recurrence relations for the Gegenbauer polynomials, after the integral on time is performed. Therefore, the above results present a good check for the time dependence of the multipole fields deduced here.

A simplified model, often used in connection with multiphonon excitations, is the harmonic vibrator model. In this model, the resonance widths are neglected and the coupled-channel equations can be solved exactly, in terms of the first-order excitation amplitudes [1]. The excitation amplitude of the nth harmonic oscillator state, for any time t, is given by

$$a_{\mathrm{h.o.}}^{(n)}(t)=\frac{[a_{1\mathrm{st}}(t)]^n}{\sqrt{n!}}\ \exp\{-|a_{1\mathrm{st}}(t)|^2/2\}, \tag{39}$$

where $a_{1\mathrm{st}}(t)$ is the excitation amplitude for the $0(\mathrm{g.s.})\rightarrow 1(one\ phonon)$ calculated with the first-order perturbation theory.

For the excitation of giant resonances, n can be identified with the state corresponding to a multiple n of the single giant resonance state. This procedure has been often used in order to calculate the cross sections for the excitation of multiphonon giant resonances. Since this result is exact in the harmonic vibrator model, it accounts for all coupling between the states. However, this result can be applied to studies of giant resonance excitation only if the same class of multipole states is involved. That is, if one considers only electric dipole excitations, and use the harmonic oscillator model, one can calculate the excitation probabilities, and cross sections, of the GDR, double GDR, triple GDR, etc. Equation (39) is not valid if the excitation of other multipolarities are involved, e.g., if the excitation of dipole states and quadrupole states are treated simultaneously. In Ref. [12] a hybrid harmonic oscillator model has been used. In this work, it is assumed that the difference between the amplitudes obtained with the harmonic oscillator model and with nth order perturbation theory is due to the appearence of the exponential term on the rhs of Eq. (39). This exponential takes care of the decrease in the occupation amplitude of the ground state as a function of time. As argued in Ref. [12], the presence of other multipole states, e.g., of quadrupole states, together with dipole states, may be accounted for by adding the first order excitation amplitudes for the quadrupole states to the exponent in Eq. (39). This would correct for the flux from the ground state to the quadrupole states. In other words, Eq. (39) should be corrected to read

$$a_{\mathrm{h.o.}}^{(n)}(\pi\lambda,t)=\frac{[a_{1\mathrm{st}}(\pi\lambda,t)]^n}{\sqrt{n!}}$$
$$\times\exp\left\{-\sum_{\pi'\lambda'}|a_{1st}(\pi'\lambda',t)|^2/2\right\}. \tag{40}$$

The harmonic oscillator model is not in complete agreement with the experimental findings. The double-GDR and double-GQR states do not have exactly twice the energy of the respective GDR and GQR states [2,3]. Apparently, the matrix elements for the transition from the GDR (GQR) to the double-GDR (double-GQR) state does not follow the boson-rule [13] (see end of Sec. III). This is borne out by the discrepancy between the experimental cross sections for the excitation of the double GDR and the double GQR with the perturbation theory, and with the harmonic oscillator model [2,3]. Thus a coupled-channels calculation is useful to determine which matrix elements for the transitions among the giant resonance states reproduce the experimental data.

B. Nuclear excitation and strong absorption

In peripheral collisions the nuclear interaction between the ions can also induce excitations. This can be easily calculated in a vibrational model. The amplitude for the excitation of a vibrational mode by the nuclear interaction in relativistic heavy ion collisions can be obtained assuming that a residual interaction U between the projectile and the target exists, and that it is weak. According to the Bohr-Mottelson particle-vibrator coupling model, the matrix element for the transition $i\rightarrow f$ is given by

$$V_{fi}^{N(\lambda\mu)}(\mathbf{r})\equiv\langle I_f M_f|U|I_i M_i\rangle$$
$$=\frac{\delta_\lambda}{\sqrt{2\lambda+1}}\langle I_f M_f|Y_{\lambda\mu}|I_i M_i\rangle Y_{\lambda\mu}(\hat{\mathbf{r}})U_\lambda(r), \tag{41}$$

where $\delta_\lambda=\beta_\lambda R$ is the vibrational amplitude, or *deformation length*, R is the nuclear radius, and $U_\lambda(r)$ is the transition potential.

The deformation length δ_λ can be directly related to the reduced matrix elements for electromagnetic transitions. Using well-known sum rules for these matrix elements one finds a relation between the deformation length and the nuclear masses and sizes. For isoscalar excitations one gets [14]

$$\delta_0^2 = 2\pi \frac{\hbar^2}{m_N \langle r^2 \rangle} \frac{1}{AE_x}, \quad \delta_{\lambda \geq 2}^2 = \frac{2\pi}{3} \frac{\hbar^2}{m_N} \lambda(2\lambda+1) \frac{1}{AE_x}, \tag{42}$$

where A is the atomic number, $\langle r^2 \rangle$ is the rms radius of the nucleus, and E_x is the excitation energy.

The transition potentials for nuclear excitations can be related to the optical potential in the elastic channel. The basic idea is that the interaction between the projectile and the target induces surface vibrations in the target. Only the contact region between the nuclei in grazing collisions is of relevance. One thus expects that the interaction potential is proportional to the derivatives of the optical potential in the elastic channel, which peak at the surface. This is discussed in details in Ref. [14]. The transition potentials for isoscalar excitations are

$$U_0(r) = 3U_{\rm opt}(r) + r \frac{dU_{opt}(r)}{dr}, \tag{43}$$

for monopole, and

$$U_2(r) = \frac{dU_{\rm opt}(r)}{dr}, \tag{44}$$

for quadrupole modes.

For dipole isovector excitations

$$\delta_1 = \frac{\pi}{2} \frac{\hbar^2}{m_N} \frac{A}{NZ} \frac{1}{E_x}, \tag{45}$$

where Z (N) the charge (neutron) number. The transition potential in this case is [14]

$$U_1(r) = \chi \left(\frac{N-Z}{A} \right) \left(\frac{dU_{\rm opt}}{dr} + \frac{1}{3} R_0 \frac{d^2 U_{\rm opt}}{dr^2} \right), \tag{46}$$

where the factor χ depends on the difference between the proton and the neutron matter radii as

$$\chi \frac{2(N-Z)}{3A} = \frac{R_n - R_p}{\frac{1}{2}(R_n + R_p)} = \frac{\Delta R_{np}}{R_0}. \tag{47}$$

Thus the strength of isovector excitations increases with the difference between the neutron and the proton matter radii. This difference is accentuated for neutron-rich nuclei and should be a good test for the quantity ΔR_{np} which enters the above equations.

The time dependence of the matrix elements above can be obtained by making a Lorentz boost. Since the potentials $U_\lambda[r(t)]$ peak strongly at $t=0$, we can safely approximate $\theta(t) \simeq \theta(t=0) = \pi/2$ in the spherical harmonic of Eq. (41). One gets

TABLE I. Parameters [16] for the nucleon-nucleon amplitude, $f_{NN}(\theta=0°) = (k_{NN}/4\pi)\ \sigma_{NN}(i+\alpha_{NN})$.

E [MeV/nucl]	σ_{NN} [fm^2]	α_{NN}
85	6.1	1
94	5.5	1.07
120	4.5	0.7
200	3.2	0.6
342.5	2.84	0.26
425	3.2	0.36
550	3.62	0.04
650	4.0	−0.095
800	4.26	−0.075
1000	4.32	−0.275
2200	4.33	−0.33

$$V_{fi}^{N(\lambda\mu)}(\mathbf{r}) \equiv \langle I_f M_f | U | I_i M_i \rangle = \gamma \frac{\delta_\lambda}{\sqrt{2\lambda+1}} \langle I_f M_f | Y_{\lambda\mu} | I_i M_i \rangle Y_{\lambda\mu} \left(\theta = \frac{\pi}{2} \right) \times U_\lambda[r(t)], \tag{48}$$

where $r(t) = \sqrt{b^2 + \gamma^2 v^2 t^2}$.

Using the Wigner-Eckart theorem, the matrix element of the spherical harmonics becomes

$$\langle I_f M_f | Y_{\lambda\mu} | I_i M_i \rangle = (-1)^{I_f - M_f} \left[\frac{(2I_i+1)(2\lambda+1)}{4\pi(2I_f+1)} \right]^{1/2} \begin{pmatrix} I_f & \lambda & I_i \\ -M_f & \mu & M_i \end{pmatrix} \times \begin{pmatrix} I_f & \lambda & I_i \\ 0 & 0 & 0 \end{pmatrix}. \tag{49}$$

For high energy collisions, the optical potential $U(r)$ can be constructed by using the t-$\rho\rho$ approximation [15]. One gets

$$U(r) = -\frac{\hbar v}{2} \sigma_{NN}(\alpha_{NN} + i) \int \rho_1(\mathbf{r}') \rho_2(\mathbf{r} - \mathbf{r}') d^3 r', \tag{50}$$

where σ_{NN} is the nucleon-nucleon cross section, and α_{NN} is the real-to-imaginary ratio of the forward ($\theta = 0°$) nucleon-nucleon scattering amplitude. A set of the experimental values of these quantities, useful for our purposes, is given in Table I.

We are not interested here in diffraction and refraction effects in the scattering, but on the excitation probabilities for a given impact parameter. The strong absorption occurring in collisions with small impact parameters can be included. This can be done by using the eikonal approximation and the optical potential, given by Eq. (50). The practical result is that the excitation probabilities for a given impact

parameter b, including the sum of the nuclear and the Coulomb contributions to the excitation, are given by

$$P_{fi}(b)=|a_{fi}^{C}(b)+a_{fi}^{N}(b)|^2 \times \exp\left\{-\sigma_{NN}\int dz \int d^3r\,\rho_1(\mathbf{r}')\rho_2(\mathbf{r}-\mathbf{r}')\right\}, \tag{51}$$

where $r=\sqrt{b^2+z^2}$. The corresponding excitation cross sections are obtained by an integration of the above equation over impact parameters.

III. THE EFFECT OF FINITE RESONANCE WIDTHS

Up to now we have assumed that the excited states are isolated states, with zero width. However, this assumption is not realistic and it is important to study the effect of finite resonance widths on the excitation amplitudes. This is specially relevant for the case of excitation of giant resonances, which have a broad structure. The simplest way to study this effect is by using the coupled-channels Born approximation. This approximation was used in Ref. [6] to describe the excitation of the double giant resonance in relativistc heavy ion collisions. It is based on the idea that in such cases only the coupling between the ground state and the dominant giant dipole state has to be treated exactly. The reason is that the transitions to giant quadrupole and to the double-phonon states have low probability amplitudes, even for small impact parameters. However, an exact treatment of the back-and-forth transitions between the ground state and the giant dipole state is necessary. This leads to modifications of the transitions amplitudes to the remaining resonances, which are populated by the ground state and the GDR. In Ref. [6] the application of the method was limited to the use of an schematic interaction, and the magnetic substates were neglected. These deficiencies are corrected here. The method allows the inclusion of the width of the giant resonances in a very simple and straightforward way. It will be useful for us to compare with the coupled-channels calculations with isolated states, as we described in the previous sections. Figure 1 represents our procedure. The GDR is coupled to the ground state while the remaining resonances are fed by these two states according to first order perturbation theory. The coupling matrix elements involves the ground state and a set of doorway states $|D_{\lambda\mu}^{(n)}\rangle$, where n specifies the kind of resonance and $\lambda\mu$ are angular momentum quantum numbers. The amplitudes of these resonances in real continuum states are

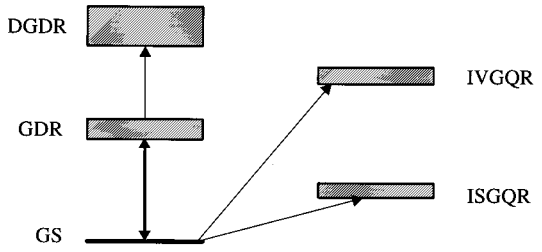

FIG. 1. Schematic representation of the excitation of giant resonances, populated in heavy ion collisions.

$$\alpha^{(n)}(\epsilon)=\langle\phi(\epsilon)|D_{\lambda\mu}^{(n)}\rangle, \tag{52}$$

where $\phi(\epsilon)$ denotes the wave function of one of the numerous states which are responsible for the broad structure of the resonance. In this equation $\epsilon=E_x-E_n$, where E_x is the excitation energy and E_n is the centroid of the resonance considered.

As we have stated above, in this approach we use the coupled-channels equations for the coupling between the ground state and the GDR. This results in the following coupled-channels equations:

$$i\hbar\dot{a}_0(t)=\sum_\mu \int d\epsilon\langle\phi(\epsilon)|D_{1\mu}^{(1)}\rangle\langle D_{1\mu}^{(1)}V_{E1,\mu}(t)|0\rangle\exp\left\{-\frac{i}{\hbar}(E_1+\epsilon)t\right\}a_{\epsilon,1\mu}^{(1)}(t) =\sum_\mu \int d\epsilon\,\alpha^{(1)}(\epsilon)V_\mu^{(01)}(t)\exp\left\{-\frac{i}{\hbar}(E_1+\epsilon)t\right\}a_{\epsilon,1\mu}^{(1)}(t), \tag{53}$$

and

$$i\hbar\dot{a}_{\epsilon,1\mu}^{(1)}(t)=[(\alpha^{(1)}(\epsilon)V_\mu^{(01)}(t)]^*\ \exp\{i(E_1+\epsilon)t/\hbar\}a_0(t). \tag{54}$$

Above, $(n=1)$ stands for the GDR, a_0 denotes the occupation amplitude of the ground state and $a_{\epsilon,1\mu}^{(1)}$ the occupation amplitude of a state located at an energy ϵ away from the GDR centroid, and with magnetic quantum number μ $(\mu=-1,0,1)$. We used the shorthand notation $V_\mu^{(01)}(t)=\langle D_{1\mu}^{(1)}|V_{E1,\mu}(t)|0\rangle$.

Integrating Eq. (54) and inserting the result in Eq. (53), we get the integro-differential equation for the ground state occupation amplitude

$$\dot{a}_0(t)=-\frac{1}{\hbar^2}\sum_\mu V_\mu^{(01)}(t)\int d\epsilon|\alpha^{(1)}(\epsilon)|^2\int_{-\infty}^{t}dt'[V_\mu^{(01)}(t')]^* \times\exp\{-i(E_1+\epsilon)(t-t')/\hbar\}a_0(t'), \tag{55}$$

where we used that $a_{\epsilon,1\mu}^{(1)}(t=-\infty)=0$. To carry out the inte-

gration over ϵ, we should use an appropriate parametrization for the doorway amplitude $\alpha^{(1)}(\epsilon)$. A convenient choice is the Breit-Wigner (BW) form

$$|\alpha^{(1)}(\epsilon)|^2=\frac{1}{2\pi}\left[\frac{\Gamma_1}{\epsilon^2+\Gamma_1^2/4}\right], \tag{56}$$

where Γ_1 is chosen to fit the experimental width. In this case, this integral will be the simple exponential

$$\int d\epsilon|\alpha^{(1)}(\epsilon)|^2 \exp\left\{-i\frac{(E_1+\epsilon)t}{\hbar}\right\}$$

$$=\exp\left\{-i\frac{(E_1-i\Gamma_1/2)t}{\hbar}\right\}. \tag{57}$$

A better agreement with the experimental line shapes of the giant resonances is obtained by using a Lorentzian (L) parametrization for $|\alpha^{(1)}(\epsilon)|^2$, i.e.,

$$|\alpha^{(1)}(\epsilon)|^2=\frac{2}{\pi}\left[\frac{\Gamma_1 E_x^2}{(E_x^2-E_1^2)^2+\Gamma_1^2E_x^2}\right], \tag{58}$$

where $E_x=E_1+\epsilon$. The energy integral can still be performed exactly [11] but now it leads to the more complicated result

$$\int d\epsilon|\alpha^{(1)}(\epsilon)|^2 \exp\left\{-i\frac{(E_1+\epsilon)t}{\hbar}\right\}$$

$$=\left(1-i\frac{\Gamma_1}{2E_1}\right)\exp\left\{-i\frac{(E_1-i\Gamma_1/2)t}{\hbar}\right\}+\Delta C(t), \tag{59}$$

where $\Delta C(t)$ is a nonexponential correction to the decay. For the energies and widths involved in the excitation of giant resonances, this correction can be shown numerically to be negligible. It will therefore be ignored in our subsequent calculations. After integration over ϵ, Eq. (55) reduces to

$$\dot a_0(t)=-\mathscr{S}_1\sum_\mu V_\mu^{(01)}(t)\int_{-\infty}^{t}dt'[V_\mu^{(01)}(t')]^*$$

$$\times\exp\left\{-i\frac{(E_1-i\Gamma_1/2)(t-t')}{\hbar}\right\}a_0(t'), \tag{60}$$

where the factor $\mathscr{S}_1$ is $\mathscr{S}_1=1$ for BW shape and $\mathscr{S}_1=1-i\Gamma_1/2E_1$ for L shape.

We can take advantage of the exponential time dependence in the integrand of the above equation, to reduce it to a set of second order differential equations. Introducing the auxiliary amplitudes $A_\mu(t)$, given by the relation

$$a_0(t)=1+\sum_\mu A_\mu(t), \tag{61}$$

with initial conditions $A_\mu(t=-\infty)=0$, and taking the derivative of Eq. (60), we get

$$\ddot A_\mu(t)-\left[\frac{\dot V_\mu^{(01)}(t)}{V_\mu^{(01)}(t)}-\frac{i}{\hbar}\left(E_1-i\frac{\Gamma_1}{2}\right)\right]\dot A_\mu(t)$$

$$-\mathscr{S}_1\frac{|V_\mu^{(01)}(t)|^2}{\hbar^2}\left[1+\sum_{\mu'}A_{\mu'}(t)\right]=0. \tag{62}$$

Solving the above equation, we get $a_0(t)$. Using this amplitude and integrating Eq. (54), one can evaluate $a^{(1)}_{\epsilon,1\mu}(t)$. The probability density for the population of a GDR continuum state with energy E_x in a collision with impact parameter b, $P_1(b,E_x)$, is obtained through the summation over the asymptotic ($t\to\infty$) contribution from each magnetic substate. We get

$$P_1(b,E_x)=|\alpha^{(1)}(E_x-E_1)|^2$$

$$\times\sum_\mu\left|\int_{-\infty}^{\infty}dt'\ \exp\{iE_xt'\}\right.$$

$$\left.\times[V_\mu^{(01)}(t')]^*a_0(t')\right|^2, \tag{63}$$

where $|\alpha^{(1)}(E_x-E_1)|^2$ is given by Eq. (56) or by Eq. (58), depending on the choice of the resonance shape.

To first order, DGDR continuum states can be populated through $E2$ coupling from the ground state or through $E1$ coupling from GDR states. The probability density arising from the former is given by Eq. (63), with the replacement of the line shape $|\alpha^{(1)}|^2$ by its DGDR counterpart $|\alpha^{(2)}|^2$ (defined in terms of parameters E_2 and Γ_2) and the use of the appropriate coupling-matrix elements $V_\mu^{(02)}(t)$ with the $E2$ time dependence given by (29). On the other hand, the contribution from the latter process is

$$P_2(b,E_x)=|\alpha^{(2)}(E_x-E_2)|^2\mathscr{S}_1\sum_\nu\left|\int_{-\infty}^{\infty}dt'\ \exp\{iE_xt'\}\sum_\mu\ [V_{\nu\mu}^{(12)}(t')]^*\int_{-\infty}^{t'}dt''[V_\mu^{(01)}(t'')]\right.$$

$$\left.\times\exp\left\{-i\frac{(E_1-i\Gamma_1/2)(t-t')}{\hbar}\right\}a_0(t'')\right|^2, \tag{64}$$

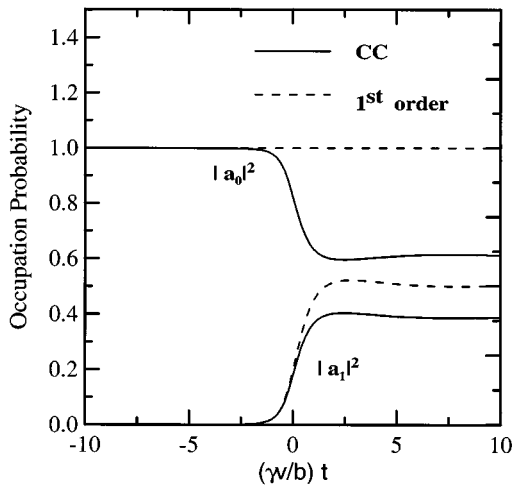

FIG. 2. Time dependence of the occupation probabilities $|a_0|^2$ and $|a_1|^2$, in a collision with impact parameter $b=15$ fm. The time is measured in terms of the dimensionless variable $\tau=(v\gamma/b)t$. The system is ^{208}Pb (640 MeV A) + ^{208}Pb.

We should point out that Eq. (64) is *not* equivalent to second-order perturbation theory. This would be true only in the limit $a_0(t)\rightarrow 1$. In our approach, $a_0(t)\neq 1$, since it is modified by the time-dependent coupling to the GDR state. This coupling is treated exactly by means of the coupled-channels equations. We consider that this is the main effect on the calculation of the DGDR (double giant dipole resonance) excitation probability. This approach is justified due to the small excitation amplitude for the transition $1\rightarrow 2$, since $a_1(t)\ll a_0(t)$.

Equations similar to (63) can also be used to calculate the ISGQR (isoscalar giant quadrupole resonance) and IVGQR (isovector giant quadrupole resonance) excitation probabilities, with the proper choice of energies, widths, and transition potentials [e.g., $V_{E2}(t)$, or $V_{N2}(t)$, or both].

In the next section we will apply the results of Secs. II A, II B, and III, to analyze some examples of relativistic nuclear and Coulomb excitation.

IV. APPLICATIONS

We consider the excitation of giant resonances in ^{208}Pb projectiles, incident on ^{208}Pb targets at 640 A MeV. This reaction has been recently studied at the GSI/SIS, Darmstadt [2]. For this system the excitation probabilities of the isovector giant dipole (IVGD) at 13.5 MeV are large and, consequently, high order effects of channel coupling should be relevant. To assess the importance of these effects, we assume that the GDR state depletes 100% of the energy-weighted sum rule and neglect the resonance width. The influence of resonance widths will be considered later, in Sec. IV B.

A. Zero-width calculations

As a first step, we study the time evolution of the excitation process, solving the coupled-channels equations for a reduced set of states. We consider only the ground state (g.s.) and the GDR. The excitation probability is then compared with that obtained with first order perturbation theory. This is done in Fig. 2, where we plot the occupation probabilities of the g.s., $|a_0(t)|^2$, and of the GDR, $|a_1(t)|^2$, as functions of time, for a collision with impact parameter $b=15$ fm. As discussed earlier, the Coulomb interaction is strongly peaked around $t=0$, with a width of the order $\Delta t\simeq b/\gamma v$. Accordingly, the amplitudes are rapidly varying in this time range. A comparison between the CC calculation (solid line) and first order perturbation theory (dashed line) shows that the high order processes contained in the former lead to an appreciable reduction of the GDR excitation probability. From this figure we can also conclude that our numerical calculations can be restricted to the interval $-10<\tau<10$, where $\tau=(\gamma v/b)t$ is the time variable measured in natural units. Outside this range, the amplitudes reach asymptotic values.

TABLE II. Excitation cross sections (in milibarns) of the IVGDR, and of the $n\times$GDR states in the reaction ^{208}Pb+^{208}Pb at 640 MeV A. A comparison with first order perturbation theory and the harmonic oscillator is made.

State	1st pert. th.	Harm. osc.	c.c.
IVGD	3891	3235	3210
$2\otimes$IVGD	388	281	280
$3\otimes$IVGD	39.2	27.3	32.7
$4\otimes$IVGD	4.2	2.4	3.2

It is worthwhile to compare the predictions of first order perturbation theory with those of the harmonic oscillator model and the CC calculations. In addition to the GDR, we include the following multiphonon states: a double giant dipole state ($2\otimes$IVGD) at 27 MeV, a triple giant dipole state ($3\otimes$IVGD) at 40.5 MeV, and a quadruple giant dipole state ($4\otimes$IVGD) at 54 MeV. The coupling between the multiphonon states are determined by boson factors, as explained at the end of Sec. II B. Direct excitations of the multiphonon states from the g.s. are not considered. The angular momentum addition rules for bosons yields the following angular momentum states: $L=0$ and 2, for the $2\otimes$GDR state; $L=1$, 2, and 3, for the $3\otimes$GDR state; and $L=0$, 1, 2, 3, and 4, for the $4\otimes$GDR state. We assume that states with the same number of phonons are degenerate. In Table II, we show the resulting cross sections. The excitation probabilities and the cross section were calculated with the formalism of Sec. II. The integration over impact parameter was carried out in the interval $b_{\min}<b<\infty$. As we discuss below, the low-b cut-off value [13] $b_{\min}=14.3$ fm mocks up absorption effects. We have checked that the CC results are not significantly affected by the unknown phases of the transition matrix elements. Since the multiphonon spectrum is equally spaced,

TABLE III. Transition probabilities at $b=14.3$ fm, for the reaction ^{208}Pb+^{208}Pb at 640 MeV A. A comparison with first order perturbation theory is made.

Trans.	1st pert. th.	c.c.
g.s.$\rightarrow$g.s.		0.515
g.s.$\rightarrow$IVGD	0.506	0.279
g.s.$\rightarrow$ISGQ	0.080	0.064
g.s.$\rightarrow$IVGQ	0.064	0.049
g.s.$\rightarrow 2\otimes$IVGD	0.128	0.092

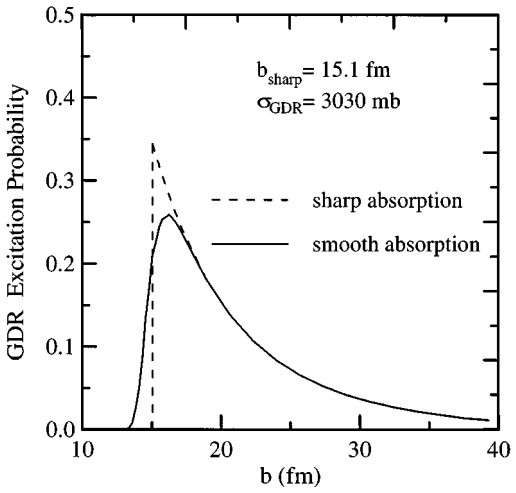

FIG. 3. The GDR excitation probabilities as functions of the impact parameter, for sharp and smooth absorptions. The system is ^{208}Pb (640 MeV A) + ^{208}Pb.

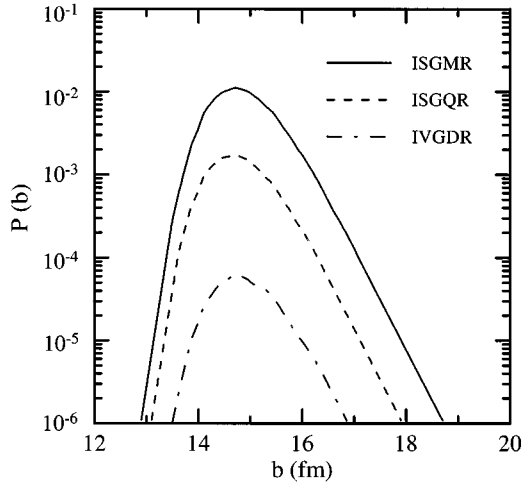

FIG. 4. Nuclear excitation probabilities as functions of the impact parameter. The system is ^{208}Pb (640 MeV A) + ^{208}Pb.

and the coupling matrix elements are related through boson factors (see the end of Sec. II B), the harmonic oscillator and the CC cross sections should be equal. In fact the numerical results of these calculations given in the table are very close. We also see that the excitation cross sections of triple- and quadruple-phonon states are much smaller than that for the $2\otimes$GDR. Therefore, we shall concentrate our studies on the $2\otimes$GDR, neglecting other multiphonon states.

Next, we include the remaining important giant resonances in ^{208}Pb. Namely, the isoscalar giant quadrupole (ISGQ) at 10.9 MeV and the isovector giant quadrupole (IVGQ) at 22 MeV. Also in this case, we use 100% of the energy-weighted sum rules to deduce the strength matrix elements. In Table III, we show the excitation probabilities in a grazing collision, with $b=14.3$ fm. We see that first order perturbation theory yields a very large excitation probability for the IVGD state. This is strongly reduced in a coupled channels (c.c.) calculation, as we have already discussed in connection with the Fig. 2. The excitations of the remaining states are also influenced. They are reduced due to the lowering of the occupation probabilities of the g.s. and of the IVGD state in the c.c. calculation. As expected, perturbation theory and c.c. calculations agree at large impact parameters, when the transition probabilities are small. For the excitation of the $2\otimes$IVGD state we used second-order perturbation theory to obtain the value in the second column. The presence of the ISGQR and the IVGQR influence the c.c. probabilities for the excitation of the GDR and the $2\otimes$IVGD, respectively.

We should also consider the effects of strong absorption in grazing collisions, as discussed in Sec. II B. In Fig. 3 we plot the GDR excitation probability as a function of the impact parameter. In the solid line, we consider absorption according to Eq. (51). In the construction of the optical potential we used the g.s. densities calculated from the droplet model of Myers and Swiatecki [17]. As shown in Ref. [1], this parametrization yields the best agreement between experiment and theory. The dashed line does not include absorption. To simulate strong absorption at low impact parameters, we use $b_{\min}=15.1$ fm as a lower limit in the impact parameter integration of Eq. (5). This value was chosen such as to lead to the same cross section as that obtained from the solid line.

In Fig. 4, we plot the nuclear contributions to the excitation probability, and as a function of the impact parameter. We study the excitation of the isoscalar giant monopole resonance (ISGMR), the IVGDR, and the ISGQR. The ISGMR in ^{208}Pb is located at 13.8 MeV. As discussed previously, isovector excitations are suppressed in nuclear excitation processes, due to the approximate charge independence of the nuclear interaction. We use the formalism of Sec. II B, with the deformation parameters such that 100% of the sum rule is exhausted. This corresponds to the monopole amplitude $\alpha_0=0.054$. The IVGDR and ISGQR deformation parameters are $\delta_1=0.31$ fm and $\delta_2=0.625$ fm, respectively. The IVGQR excitation probability is much smaller than the other excitation probabilities and is, therefore, not shown.

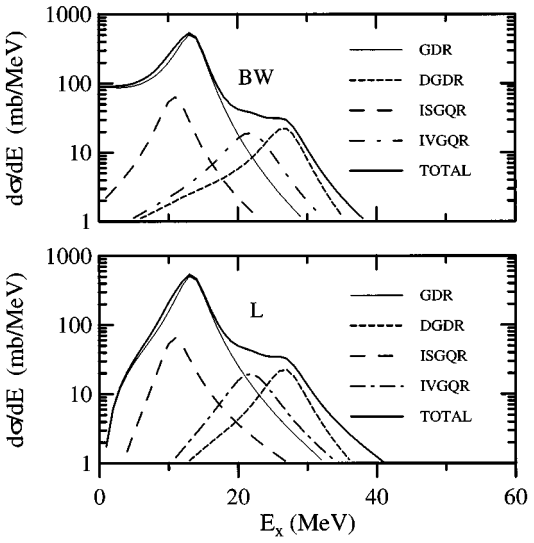

FIG. 5. Excitation energy spectra of the main giant resonances for both Breit-Wigner and Lorentzian line shapes. The system is ^{208}Pb (640 MeV A) + ^{208}Pb.

TABLE IV. Centroid energies and widths of the main giant resonances in ^{208}Pb.

	GDR	DGDR	ISGQR	IVGQR
E_r (MeV)	13.5	27.0	10.9	20.2
Γ (MeV)	4.0	5.7	4.8	5.5

The nuclear excitation is peaked at the grazing impact parameter and is only relevant within an impact parameter range of ~ 2 fm. Comparing to Fig. 3, we see that these excitation probabilities are orders of magnitude smaller than those for Coulomb excitation. Consequently, the corresponding cross sections are much smaller. We get 14.8 mb for the isoscalar GDR, 2.3 mb for the ISGQR, and 2.3 mb for the IVGDR. The interference between the nuclear and the Coulomb excitation is also small and can be neglected.

B. Effect of resonance widths

We now turn to the influence of the giant resonance widths on the excitation dynamics. We use the CCBA formalism developed in Sec. III. Schematically, the CC problem is that represented Fig. 1. As we have seen above, the strongest coupling occurs between the g.s. and the GDR.

In Fig. 5, we show the excitation energy spectrum for the GDR, the DGDR (a shorthand notation for the $2\otimes$IVGD), ISGQR and IVGQR. The centroid energies and the widths of these resonances are listed in Table IV. The figure shows excitation spectra obtained with both Breit-Wigner (BW) and Lorentzian (L) line shapes. One observes that the BW and L spectra have similar strengths at the resonance maxima. However, the low energy parts (one or two widths below the centroid) of the spectra are more than one order of magnitude higher in the BW calculation. The reason for this behavior is that Coulomb excitation favors low energy transitions and the BW has a larger low energy tail as compared with the Lorentzian line shape. The contribution from the DGDR leads to a pronounced bump in the total energy spectrum. This bump depends on the relative strength of the DGDR with respect to the GDR. In Fig. 6, we show the ratio $\sigma_{\rm DGDR}/\sigma_{\rm GDR}$ as a function of the bombarding energy. We observe that this ratio is roughly constant in the energy range $E_{\rm lab}/A = 200-1000$ MeV and it falls beyond these limits. This range corresponds to the SIS energies at the GSI-Darmstadt facility.

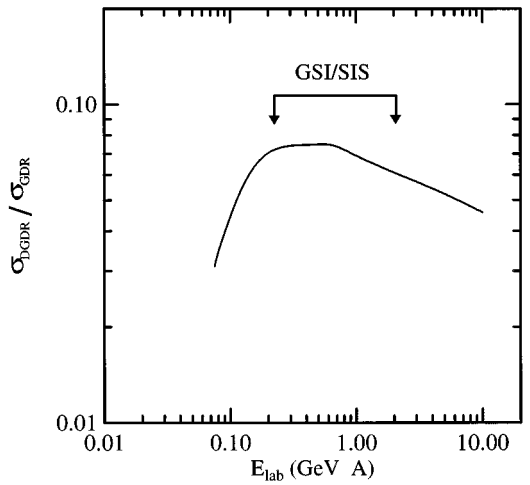

FIG. 6. Ratio between the DGDR and the GDR cross sections in ^{208}Pb + ^{208}Pb collisions, as a function of the bombarding energy.

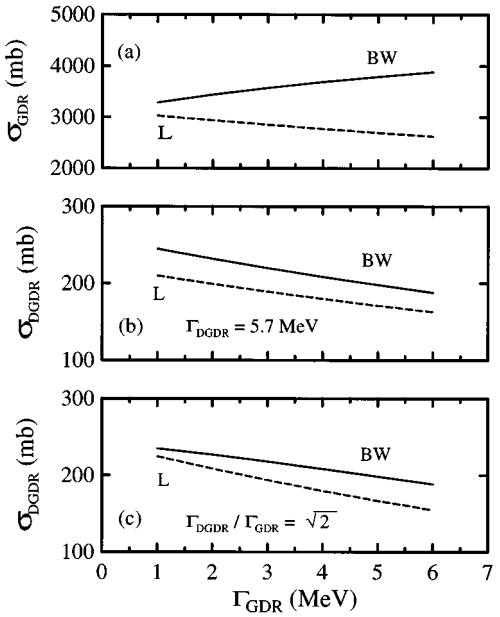

FIG. 7. Dependence of $\sigma_{\rm GDR}$ and $\sigma_{\rm DGDR}$ on the GDR width, treated as a free parameter. For details see the text. The system is ^{208}Pb (640 MeV A) + ^{208}Pb.

We now study the influence of the resonance widths and shapes on the GDR and DGDR cross sections. This study is similar to that presented in Ref. [6], except that we now have a realistic three dimensional treatment of the states and consider different line shapes. In the upper part of Fig. 7, denoted by (a), we show $\sigma_{\rm GDR}$ as a function of $\Gamma_{\rm GDR}$, treated as a free parameter. We note that the BW and L parametrizations lead to different trends. In the BW case the cross section grows with $\Gamma_{\rm GDR}$ while in the L case it decreases. The growing trend is also found in Ref. [6], which uses the BW line shape. The reason for this trend in the BW case is that an increase in the GDR width enhances the low energy tail of the line shape, picking up more contributions from the low energy transitions, favored in Coulomb excitation. On the other hand, an increase of the GDR width enhances the doorway amplitude to higher energies where Coulomb excitation is weaker. In Figs. 7(b) and 7(c), we study the dependence of $\sigma_{\rm GDR}$ on $\Gamma_{\rm GDR}$. In Fig. 7(b), the DGDR width is kept fixed at the value 5.7 MeV while in Fig. 7(c) it is kept proportional to $\sigma_{\rm GDR}$, fixing the ratio $\Gamma_{\rm DGDR}/\Gamma_{\rm GDR} = \sqrt{2}$.

TABLE V. Cross sections in milibarns for the excitation of giant resonances in lead, for the reaction ^{208}Pb+^{208}Pb at 640 MeV A.

GDR	DGDR	ISGQR	IVGQR
2704	184 (199) [198]	347	186

The first point to be noticed is that the BW results are systematically higher than the L ones. This is a consequence of the different low energy tails of these functions, as discussed above. One notices also that σ_{DGDR} decreases with Γ_{GDR} both in the BW and L cases. This trend can be understood in terms of the uncertainty principle. If the GDR width is increased, its lifetime is reduced. Since the DGDR is dominantly populated from the GDR, its short lifetime leads to decay before the transition to the DGDR.

To assess the sensitivity of the DGDR cross section on the strength of the matrix elements and on the energy position of the resonance, we present in Table V the cross sections for the excitation of the GDR, DGDR, ISGQR, and IVGQR, obtained with the CCBA approximation and 100% of the sum rules for the respective modes. In this calculation we have included the strong absorption, as explained in Sec. II B. For comparison, the values inside parenthesis (and brackets) of the DGDR excitation cross section include a direct excitation of the $L=2$ DGDR state. We assumed that 20% of the $E2$ sum rule could be allocated for this excitation mode of the DGDR. The cross sections increase by less than 10% in this case. The value inside parenthesis (brackets) assume a positive (negative) sign of the matrix element for the direct excitation.

Since the excitation of the DGDR is weak, it is very well described by Eq. (64) and the DGDR population is approximately proportional to the squared strength of $V^{(12)}$. Therefore, to increase the DGDR cross section by a factor of 2, it is necessary to violate the relation of Eq. (35) by the same factor. This would require a strongly anharmonic Hamiltonian for the nuclear collective modes, which would not be supported by traditional nuclear models [13]. Arguments supporting such anharmonicities have recently been presented in Ref. [18]. Another effect arising from anharmonicity would be the spin or isospin splitting of the DGDR. Since the Coulomb interaction favors lower energy excitations, it is clear that a decrease of the DGDR centroid would increase its cross section. A similar effect would occur if a strongly populated substate is splitted to lower energies. To study this point, we have varied the energy of the DGDR centroid in the range $20\ \mathrm{MeV} \leqslant E_{\mathrm{DGDR}} \leqslant 27\ \mathrm{MeV}$. The obtained DGDR cross sections (including direct excitations) are equal to 620 mb, 299 mb, and 199 mb, for the centroid energies of 20 MeV, 24 MeV, and 27 MeV, respectively. Although the experimental data on the DGDR excitation [2,3] seem to indicate that $E_{\mathrm{DGDR}} \sim 2E_{\mathrm{GDR}}$, a small deviation (in the range of 10–15 %) of the centroid energy from this value might be possible. However, the data are not conclusive, and more experiments are clearly necessary. We conclude that, from the arguments analyzed here, the magnitude of the DGDR cross section is more sensitive to the energy position of this state. The magnitude of the DGDR cross section would increase by a factor 2 if the energy position of the DGDR decreases by 20%, as found in Ref. [18].

V. DISCUSSION AND CONCLUSIONS

In this paper we investigated at great length the excitation of giant resonances in heavy-ion reactions. Both the single- and double-giant dipole resonances were considered. The effect of the finite lifetimes of these resonances on their excitation probabilities was carefully assessed. The comparison with the available experimental data shows that some physics is still missing. Here we address this issue.

In our discussion of the excitation of a damped giant resonance, the damping arises from the coupling to the large number of noncollective states that surround the GDR and shares with it its quantum numbers. One should keep in mind that our final result for the excitation probability involves an implicit average over the ''chaotic'' degrees of freedom whose quantum manifestation is just the fine structure states. At this point one is reminded of a well known fact in reaction theory, namely, ensemble or energy averaged cross sections contain two pieces: one obtained from an average amplitude, or ''optical'' piece, and a second piece which arises from the fluctuations. We expect similar contribution of the fluctuations to the excitation probability in the case of the GR. Here, however, the fluctuations are in the ''host'' nucleus and not in the compound nucleus.

At this point, we recall similar type of fluctuations which constitute the dominant piece in the case of deep inelastic heavy ion reactions [19], when it is assumed that only chaotic channels are involved in the inelastic transitions. The investigation of the effects of fluctuations on the excitation of giant resonances in heavy-ion reactions, following the procedure of [19], is underway and will be reported in a future publication.

ACKNOWLEDGMENTS

We would like to express our gratitude to Dr. Hans Emling for useful comments and suggestions during the development of this work. One of us (C.A.B.) acknowledges financial support from the GSI-Darmstadt and FAPESP. This work was supported in part by the Brazilian agencies CNPq and FINEP. This work was also partially supported by the National Science Foundation through a grant for the Institute for Theoretical Atomic and Molecular Physics at Harvard University and Smithsonian Astrophysical Observatory. The work of M.S.H. at MIT was supported in part by funds provided by the U.S. Department of Energy (DOE) under cooperative agreement DE-FC02-94ER40818, and the work at the Harvard-Smithsonian Center for Astrophysics was supported by the National Science Foundation.

[1] G. Baur and C.A. Bertulani, Phys. Lett. B **174**, 23 (1986); Phys. Rep. **163**, 299 (1988); T. Aumann, C.A. Bertulani, and K. Suemmerer, Phys. Rev. C **51**, 416 (1995).

[2] H. Emling, Prog. Part. Nucl. Phys. **33**, 729 (1994).

[3] P. Chomaz and N. Frascaria, Phys. Rep. **252**, 275 (1995).

[4] P.G. Hansen, Nucl. Phys. **A553**, 89c (1993); C.A. Bertulani, L.F. Canto, and M.S. Hussein, Phys. Rep. **226**, 282 (1993).

[5] K. Alder and A. Winther, *Coulomb Excitation* (Academic

Press, New York, 1965).
[6] L.F. Canto, A. Romanelli, M.S. Hussein, and A.F.R. de Toledo Piza, Phys. Rev. Lett. **72**, 2147 (1994).
[7] C.A. Bertulani, L.F. Canto, and M.S. Hussein, Phys. Lett. B **353**, 413 (1995).
[8] A. Winther and K. Alder, Nucl. Phys. **A319**, 518 (1979).
[9] J.D. Jackson, *Classical Electrodynamics* (Wiley, New York, 1975).
[10] A.R. Edmonds, *Angular Momentum in Quantum Mechanics* (Princeton University Press, Princeton, NJ, 1960).
[11] M.S. Hussein, M.P. Pato, and A.F.R. de Toledo Piza, Phys. Rev. C **51**, 846 (1995).
[12] J. Norbury and G. Baur, Phys. Rev. C **48**, 1915 (1993).
[13] C.A. Bertulani and V. Zelevinsky, Phys. Rev. Lett. **71**, 967 (1993); Nucl. Phys. **A568**, 931 (1994).
[14] G.R. Satchler, Nuc. Phys. **A472**, 215 (1987).
[15] M.S. Hussein, R. Rego, and C.A. Bertulani, Phys. Rep. **201**, 279 (1991).
[16] L. Ray, Phys. Rev. C **20**, 1857 (1979).
[17] W.D. Myers and W.J. Swiatecki, Ann. Phys. **55**, 395 (1969); **84**, 186 (1974).
[18] C. Volpe, F. Catara, Ph. Chomaz, M.V. Andrés and E.G. Lanza, Nucl. Phys. **A589**, 521 (1995); E.G. Lanza (private communication).
[19] D.M. Brink, J. Neto, and H.A. Weidenmuller, Phys. Lett. B **80**, 170 (1979).